

Zeno and anti-Zeno dynamics in spin-bath models

Dvira Segal, David R. Reichman

Department of Chemistry, Columbia University, 3000 Broadway, New York, NY 10027

We investigate the quantum Zeno and anti-Zeno effects in spin bath models: the spin-boson model and a spin-fermion model. We show that the Zeno-anti-Zeno transition is critically controlled by the system-bath coupling parameter, the same parameter that determines spin decoherence rate. We also discuss the crossover in a biased system, at high temperatures, and for a nonequilibrium spin-fermion system, manifesting the counteracting roles of electrical bias, temperature, and magnetic field on the spin decoherence rate.

PACS numbers: 03.65.Xp, 03.65.Yz, 05.30.-d, 31.70.Dk

The quantum Zeno effect (QZE) describes the behavior of a quantum system when frequent short time measurements inhibits decay [1, 2]. In some cases, however, the anti-Zeno effect (AZE), namely an enhancement of the decay due to frequent measurements, is observed [3, 4]. The QZE can be easily obtained for an oscillating (reversible) quantum system. When the system is unstable, the situation is more involved, and one can obtain both the QZE and AZE, depending on the interaction Hamiltonian [4], as well as the measurement interval [5]. A crossover from QZE to AZE behavior has been observed in an unstable trapped cold atomic system via a tuning of the measurement frequency [6]. Recently, Maniscalco *et al.* [7] have theoretically investigated the Zeno-anti-Zeno crossover in a model of a damped quantum harmonic oscillator. These authors demonstrated the crucial role played by the short time behavior of the environmentally induced decoherence.

In this letter we focus on spin-bath models, paradigms of quantum dissipative systems, and analyze the conditions for the occurrence of the Zeno and anti-Zeno effects. We show that the crossover between the two processes is critically controlled by the dimensionless coupling strength, as well as the temperature and the energy bias between the spin states. We also analyze the Zeno dynamics for out-of-equilibrium, electrically biased, situations. Our main result is that the same parameters which determine the extent of quantum coherence for the transient population variable, also control the Zeno-anti-Zeno transition. Therefore, the nature of spin decoherence can be predicted from the Zeno dynamics.

The models of interest here are the spin-boson model and a nonequilibrium steady state spin-fermion model, which is a simplified variant of the Kondo model. The spin-boson model, describing a two-level system coupled to a bath of harmonic oscillators, is one of the most important models for elucidating the effect of environmentally controlled dissipation in quantum mechanics [8]. The Kondo model, possibly the simplest model of a magnetic impurity coupled to an environment, describes the coupling of a magnetic atom to the conduction band electrons [9]. This system has recently regained enor-

mous interest due to significant experimental progress in mesoscopic physics [10]. For both models the prototype Hamiltonian includes three contributions

$$H = H_S + H_B + H_{SB}. \quad (1)$$

The spin system includes a two level system (TLS) with a bare tunneling amplitude Δ and a level splitting B ,

$$H_S = \frac{B}{2}\sigma_z + \frac{\Delta}{2}\sigma_x. \quad (2)$$

In what follows we refer to the bias B as a magnetic field in order to distinguish it from potential bias in a nonequilibrium system. In the bosonic case the thermal bath includes a set of independent harmonic oscillators, and the system-bath interaction is bilinear

$$\begin{aligned} H_B^{(b)} &= \sum_j \epsilon_j b_j^\dagger b_j, \\ H_{SB}^{(b)} &= \sum_j \frac{\lambda_j}{2} (b_j^\dagger + b_j) \sigma_z. \end{aligned} \quad (3)$$

b_j^\dagger, b_j are bosonic creation and annihilation operators, respectively. For a fermionic system we employ the model

$$\begin{aligned} H_B^{(f)} &= \sum_k \epsilon_k a_{k,n}^\dagger a_{k,n}, \\ H_{SB}^{(f)} &= \sum_{k,k',n,n'} \frac{V_{k,n;k',n'}}{2} a_{k,n}^\dagger a_{k',n'} \sigma_z. \end{aligned} \quad (4)$$

Here a_k^\dagger, a_k are fermionic creation and annihilation operators, and the spin interacts with n reservoirs. We also define two auxiliary Hamiltonians H_\pm as

$$H_\pm = \pm \frac{B}{2} + H_{SB}(\sigma_z = \pm) + H_B. \quad (5)$$

Note that the Hamiltonian (1) does not include explicitly the measuring device. While in Refs. [11] (boson bath) and [12] (fermion bath) the reservoirs serve as continuous detectors, here they are part of the dynamical system under measurement.

Before studying the Zeno dynamics of the dissipative systems, we briefly review the results for an isolated TLS.

For zero magnetic field, the probability to remain in the initial prepared state is given by $W(t) = \cos^2(\Delta t/2)$. The short-time dynamics ($\Delta t \ll 1$) can be approximated by $W(t) \sim 1 - (\Delta/2)^2 t^2$. If measurements are performed at regular intervals τ , the survival probability at time $t = n\tau$ becomes $W(t) \sim 1 - n(\Delta/2)^2 \tau^2 \sim \exp(-\Delta^2 \tau t/4)$. At short times an effective relaxation rate is identified as

$$\gamma_0(\tau) = (\Delta/2)^2 \tau. \quad (6)$$

As τ goes to zero, decay is inhibited, and the dynamics is frozen. This is the quantum Zeno effect.

We consider next the influence of the environment on this behavior. Within perturbation theory the dynamics of a TLS coupled to a general heat bath is given as a power series of Δ terms, $W(t) = \sum_{n=0}^{\infty} (\frac{\Delta}{2})^{2n} \Phi_n(t)$ [13]. We have numerically verified that for $\omega_c \tau \lesssim 20$, (ω_c is the reservoir cutoff frequency) the series can be approximated by the first two terms

$$\begin{aligned} W(t) &\sim 1 - 2\Re \left(\frac{\Delta}{2} \right)^2 \int_0^\tau dt_1 \int_0^{t_1} dt_2 K(t_2), \\ K(t) &= \langle e^{-iH_+ t} e^{iH_- t} \rangle, \end{aligned} \quad (7)$$

even for strong system-bath coupling [14], provided that $\Delta\tau < 1$ [15]. Here \Re denotes the Real part, the Hamiltonians H_{\pm} are defined in Eq. (5), and the trace is done over the bath degrees of freedom, irrespective of the statistics. Similarly to the isolated case, we can identify an effective decay rate at short times

$$\gamma(\tau) = \frac{\Delta^2}{2\tau} \Re \int_0^\tau dt_1 \int_0^{t_1} K(t') dt'. \quad (8)$$

In what follows we disregard the multiplicative factor $(\Delta/2)^2$. The basic question to be addressed in this letter is how does this relaxation rate depend on the system bath coupling. It is clear that when the system is decoupled from the environment, Eq. (8) reproduces the result of the isolated system, Eq. (6). For a dissipative system the central object of our calculation is therefore the correlation function $K(t)$ defined in Eq. (7). For the bosonic system (3), a standard calculation yields [16]

$$\begin{aligned} K_b(t) &= e^{-iE_s t} \exp \left\{ -\frac{1}{\pi} \int_0^\infty d\omega \frac{J(\omega)}{\omega^2} \right. \\ &\quad \times \left. [(n_\omega + 1)(1 - e^{-i\omega t}) + n_\omega(1 - e^{i\omega t})] \right\}. \end{aligned} \quad (9)$$

Here $n_\omega = [e^{\beta\omega} - 1]^{-1}$ is the Bose-Einstein distribution function, $\beta = 1/T$ is the inverse temperature, and $E_s = B + \int \frac{J(\omega)}{\pi\omega} d\omega$ is the polaron shift. The spectral density $J(\omega)$ includes the information about the system-bath interaction $J(\omega) = \pi \sum_j \lambda_j^2 \delta(\omega - \omega_j)$. For an ohmic model, $J(\omega) = 2\pi\xi\omega e^{-\omega/\omega_c}$, Eq. (9) becomes [17]

$$K_b(t) = \left(\frac{1}{1 + i\omega_c t} \right)^{2\xi} \left[\frac{\left(\frac{\pi t}{\beta} \right)}{\sinh \left(\frac{\pi t}{\beta} \right)} \right]^{2\xi} \times e^{-iE_s t} \quad (10)$$

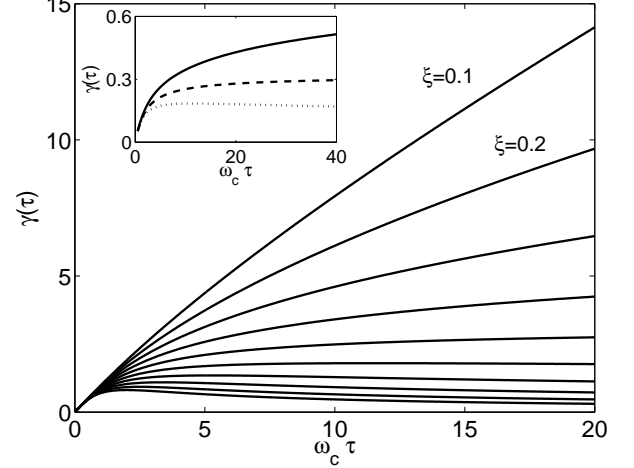


FIG. 1: The effective decay rate for a spin coupled to a bosonic bath at zero temperature for $\omega_c=1$, $E_s=0$, $\xi=0.1, 0.2, 0.3\dots 1$, top to bottom. The appearance of a maximum point in $\gamma(\tau)$ around $\omega_c\tau = 2$ for $\xi > 1/2$ marks the transition from QZE to AZE. The inset depicts the rate for $\xi=0.4$ (full), 0.5 (dashed), 0.6 (dotted), $\omega_c=10$.

where ξ is a system-bath dimensionless coupling parameter [8]. At zero temperature and for zero magnetic field, disregarding the energy shift, the effective decay rate (8) is given by ($\xi \neq \frac{1}{2}, 1$)

$$\gamma(\tau) = \frac{1 - (1 + \omega_c^2 \tau^2)^{1-\xi} \cos[2(1-\xi)\text{atan}(\omega_c \tau)]}{\tau \omega_c^2 (1-\xi)(1-2\xi)}. \quad (11)$$

The limiting behavior of this expression is

$$\gamma(\tau) \propto \begin{cases} \tau & \omega_c \tau < 1 \\ \tau^{1-2\xi} & \omega_c \tau > 1. \end{cases} \quad (12)$$

Therefore, while at very short times ($\omega_c \tau < 1$) the system always shows the QZE, irrespective of the system-bath coupling, at intermediate times $1/\omega_c < \tau < 1/\Delta$ the qualitative behavior of the decay rate crucially depends on the dimensionless coupling coefficient. The decay is inhibited (QZE) for $\xi < \frac{1}{2}$, and accelerated (AZE) for $\xi > \frac{1}{2}$. At $\xi = \frac{1}{2}$ the decay rate does not depend on

the measurement interval, $\gamma(\tau) \xrightarrow{\frac{\log(\omega_c \tau)}{\omega_c \tau} < 1} \frac{\pi \Delta^2}{4\omega_c}$. Correspondingly, at zero temperature an unbiased spin oscillates coherently at $\xi = 0$, shows damped harmonic oscillation for $0 < \xi < \frac{1}{2}$, and decays incoherently at strong dissipation, $\frac{1}{2} < \xi < 1$. At the crossover value $\xi = \frac{1}{2}$ the system can be mapped onto the Toulouse problem, describing an impurity coupled to a Fermi bath with a constant density of states. This leads to a purely Markovian exponential decay which is unaffected by measurements [18]. We therefore find that the dimensionless coupling constant ξ which controls the extent of spin decoherence, determines the occurrence of the QZE and the AZE.

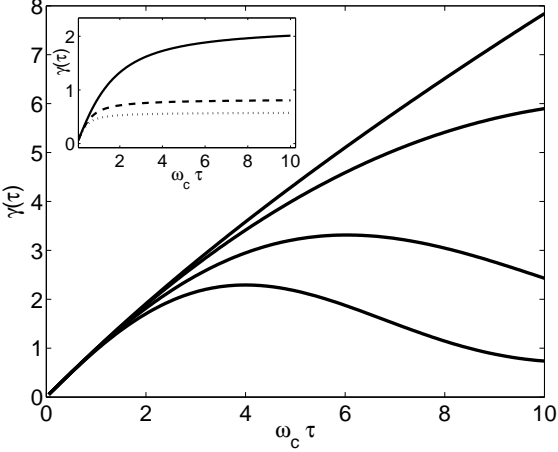


FIG. 2: The Zeno-anti-Zeno transition of a spin-boson model under a magnetic field, $T = 0K$, $\omega_c=1$, $\xi = 0.1$, $B=0$, 0.2 , 0.4 , 0.6 , top to bottom. Inset: Temperature effect, $\beta\omega_c = 0.5$, $B=0$, $\xi = 0.1$ (full), $\xi = 0.4$ (dashed), $\xi = 0.7$ (dotted).

Besides the occupation probability $W(t)$, the symmetrized equilibrium correlation function $C(t)$ is also of interest. It is unclear whether the coherent-incoherent transition of this quantity occurs at $\xi = \frac{1}{2}$ [19], or below, at $\xi = \frac{1}{3}$ [20]. Yet, since the short-time dynamics of the two-spin correlation function $C(t)$ is controlled by the same function $K(t)$ [Eq. (7)] [21], its Zeno-anti-Zeno behavior *exactly corresponds with* $W(t)$, and thus rigorously undergoes a Zeno-anti-Zeno transition at $\xi = \frac{1}{2}$.

Fig. 1 depicts the decay rate $\gamma(\tau)$ for $\xi = 0.1-1$, manifesting the crossover from the QZE to the AZE at $\xi = \frac{1}{2}$ (inset). The transition between the Zeno and anti-Zeno regimes can be manipulated by applying a finite magnetic field and by employing a finite temperature bath. Fig. 2 shows that at weak coupling, a biased system $B/\omega_c \sim 1$ tends towards a pronounced anti-Zeno behavior, in contrast to the zero magnetic field case. The influence of finite temperatures is radically different (inset): It drives the system into the Zeno regime, for all coupling strengths. This can be deducted from Eq. (9): For $\beta\omega_c < 1$, $K(t) \sim e^{-2\pi\xi t/\beta}$, and the resulting decay rate is proportional to τ at short times, saturating at $\omega_c\tau > 1$.

Our results can be elucidated by recasting the decay rate as a convolution of two memory functions,

$$\gamma(\tau) = 2 \left(\frac{\Delta}{2} \right)^2 \int_0^\infty d\omega K(\omega) F_\tau(\omega), \quad (13)$$

where the measurement function is given by $F_\tau(\omega) = \frac{\tau}{2\pi} \text{sinc}^2 \left[\frac{(\omega - E_s)\tau}{2} \right]$, and $K(\omega) = \Re \int_0^\infty e^{i\omega t} K(t) dt$, can be interpreted as the reservoir coupling spectrum [4]. Note that $K(t)$ is redefined here without the energy shift. The short-time behavior is therefore determined by the overlap of these two memory functions. For $|E_s - \omega_m| \gg 1/\tau$, with ω_m as the central frequency of $K(\omega)$, AZE takes

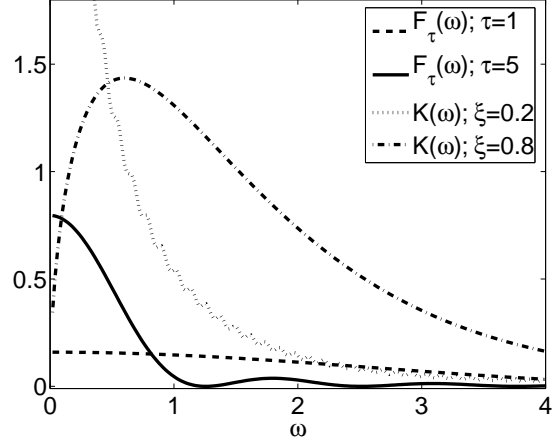


FIG. 3: The QZE and the AZE, as observed through the spectral functions $K(\omega)$ and $F_\tau(\omega)$ for $T = 0$, $\omega_c=1$, $E_s = 0$ (see Eq. (13) for definitions). Increasing ξ , $K(\omega)$ shifts towards higher frequencies overlapping poorly with $F_{\tau=5}(\omega)$, and strongly with $F_{\tau=1}(\omega)$, which leads to the AZE.

place, while for a bath with narrow coupling spectrum and for $|E_s - \omega_m| \ll 1/\tau$ the QZE occurs [4].

Fig. 3 displays $K(\omega)$ at two values: $\xi=0.2, 0.8$. We also show the measurement function $F_\tau(\omega)$ for $\omega_c\tau=1, 5$. We find that at weak coupling, the overlap between these two functions decreases upon shortening τ , leading to the QZE. In contrast, at strong coupling, since the central frequencies of $F_\tau(\omega)$ and $K(\omega)$ are detuned, increasing the width of $F_\tau(\omega)$ enhances the overlap between the functions, therefore the decay rate, leading to the AZE. This is clearly seen mathematically: At zero temperature $K(\omega) = \frac{1}{\omega_c \Gamma(2\xi)} \left(\frac{\omega}{\omega_c} \right)^{2\xi-1} e^{-\omega/\omega_c}$, with $\omega_m \sim (2\xi - 1)\omega_c$. This argument also explains the AZE observed at weak coupling for finite magnetic fields. Since $F_\tau(\omega)$ is centered around B , and $\omega_m \sim 0$ for $\xi \leq 0.5$, the AZE is expected to prevail for $B\tau > 1$, as seen in Fig. 2.

We turn now to the fermionic bath. For a single reservoir at zero temperature, and for times $D\tau > 1$, the fermionic correlation function can be calculated in the context of the Fermi-edge singularity problem [22],

$$K_f(t) \sim \frac{e^{-iBt}}{(1 + iDt)^{\delta^2/\pi^2}}. \quad (14)$$

Here $\delta = \text{atan}(\pi\rho V)$, ρ is the density of states, D is the bandwidth, the equivalent of the cutoff frequency ω_c in the bosonic case, and we used a constant coupling model $V_{k,k'} = V$. We have disregarded the energy shift coming from the diagonal coupling $V_{k,k}$, as it can always be accommodated into the external magnetic field.

Comparing Eq. (14) to the bosonic expression (10), leads to the conclusion that an unbiased spin coupled to a fermionic bath can only manifest the QZE: Since the phase shift cannot exceed $\pi/2$, the exponent in (14) is

always $\leq 1/4$, while according to Eq. (12), the AZE takes place only for larger values which are prohibited in this case. A spin coupled to more than a single lead may attain a larger exponent, which can lead to the AZE [23].

The nonequilibrium spin-fermion system, where the spin couples to *two* fermionic baths ($V_{k,n;k'n'} = V$, $n = 1, 2$) with chemical potentials shifted by $\delta\mu$, is much more interesting and involved. In this case we numerically calculate the correlation function $K_f(t)$, since its analytic form is not known at short times $Dt \leq 1$ and for arbitrary voltages [24]. This is done by expressing the zero temperature many body average as a determinant of the single particle correlation functions [16]

$$K_f(t) = \langle e^{-iH_+t} e^{iH_-t} \rangle = \det [\phi_{k,k'}(t)]_{k,k' < k_f},$$

$$\phi_{k,k'}(t) = \langle k | e^{-iH_+t} e^{iH_-t} | k' \rangle. \quad (15)$$

Here $H_{\pm} = \sum h_{\pm}$ are the single particle Hamiltonians, $|k\rangle$ are the single particle eigenstates of $H_B^{(f)}$ and the determinant is evaluated over the occupied states.

For a short-time evolution, it is satisfactory to model the fermionic reservoirs using 200 states per bath, where bias is applied by depopulating one of the reservoirs with respect to the other. The decay rate $\gamma(\tau)$, (Eq. (8)), is presented in the main plot for three situations: In the absence of both magnetic field and electric bias (full), including a finite magnetic field (dashed), and under an additional potential bias (dotted). We find that the potential bias in the fermionic system plays the role of the temperature in the bosonic environment [24], driving the anti-Zeno behavior into a Zeno dynamics.

Summarizing, we find that the same coupling parameter that monitors spin decoherence and relaxation, determines the Zeno behavior. In addition, while finite temperature and electric bias eliminate the AZE, applying a finite magnetic field can revive the effect. The relationship between the Zeno effect and spin dynamics also implies on the feasible *control* over the environment induced spin decoherence utilizing the Zeno effect, which is crucial for quantum computing applications [25].

The transition from Zeno to anti-Zeno dynamics can be controlled by modifying the environmental parameters such as the spectral density, temperature, electrical bias, and by changing the system-bath interaction, as well as the spin parameters. Trapped ions in an optical lattice is a highly versatile system possibly capable of showing the Zeno-anti-Zeno crossover. In recent years it has become feasible to trap chains of atoms, to couple them in a controlled way to the oscillatory "phonon" modes of the chain, and to probe them by a laser field [26]. Another possible setup is an atomic Bose-Einstein condensate interacting with a laser field [2]. This system is predicted to give rise to composite quasiparticles: local impurities dresses by (virtual) phonons [27]. The spin-fermion model could be realized in a semiconductor microstructure consisting of two coupled quantum dots, simulating

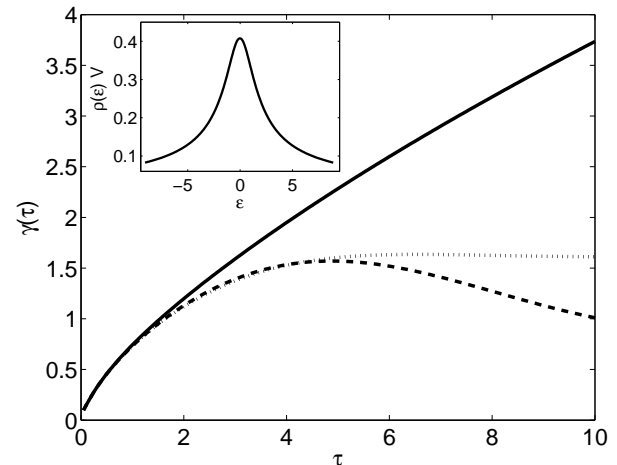


FIG. 4: The effective decay rate for a spin coupled to two fermionic baths demonstrating the counteracting roles of the magnetic field and electrical bias. $B=0$, $\delta\mu=0$ (full); $B=0.5$, $\delta\mu=0$ (dashed); $B=0.5$, $\delta\mu=0.2$ (dotted). The inset shows the Lorentzian shaped density of states.

a double-well potential, interacting with a current carrying quantum point contact (QPC) [28]. Measurements of the spin state can be done either continuously with an additional QPC, serving this time as a detector, or using laser radiation, directly detecting the population in each of the wells.

This work was supported by NSF (NIRT)-0210426.

- [1] B. Misra, E. C. G. Sudarshan, J. Math. Phys. **18**, 758 (1977).
- [2] E. W. Streed, *et al.*, Phys. Rev. Lett. **97**, 260402 (2006).
- [3] W. C. Schieve, L. P. Horwitz, J. Levitan, Phys. Lett. A **136**, 264 (1989).
- [4] A. G. Kofman, G. Kurizky, Nature **405**, 546 (2000).
- [5] P. Facchi, H. Nakazato, S. Pascazio, Phys. Rev. Lett. **86**, 2699 (2001).
- [6] M. C. Fischer, B. Gutierrez-Medina, M. G. Raizen, Phys. Rev. Lett. **87**, 040402 (2001).
- [7] S. Maniscalco, J. Piilo, K-A Suominen, Phys. Rev. Lett. **97**, 130402 (2006).
- [8] A. J. Leggett *et al.*, Rev. Mod. Phys. **59**, 1 (1987).
- [9] J. Kondo, Prog. Theo. Phys. **32**, 37 (1964).
- [10] G. A. Fiete, E. J. Heller, Rev. Mod. Phys. **75**, 933 (2003).
- [11] O. V. Prezhdo, Phys. Rev. Lett. **85**, 4413 (2000).
- [12] A. Gurvitz, Phys. Rev. B **56**, 15215 (1997).
- [13] L.-D. Chang, S. Chakravarty, Phys. Rev. B **31**, 154 (1985).
- [14] We define "strong system-bath coupling" as $\xi > 0.5$ (bosons) and $\pi\rho V \gtrsim 1$ (fermions). These parameters are defined after Eqs. (10) and (14) respectively.
- [15] In the discussion below we always assume $\Delta\tau < 1$.
- [16] G. D. Mahan, *Many-particle physics*, Plenum press, New York, (2000).
- [17] C. Aslangul, N. Pottier, D. Saint-James, Phys. Lett.

111A, 175 (1985).

[18] At the Toulouse point the polarization decay rate is $\pi\Delta^2/(2\omega_c)$ [8]. At short times our expression for the *upper level population* agrees with this value.

[19] J. T. Stockburger, C. H. Mak, Phys. Rev. Lett. **80**, 2657 (1998).

[20] F. Lesage, H. Saleur, S. Skorik, Phys. Rev. Lett. **76**, 3388 (1996).

[21] M. Sassetti, U. Weiss, Phys. Rev. A **41**, 5383 (1990).

[22] P. Nozieres, C. T. De Dominicis, Phys. Rev. **178**, 1097 (1969).

[23] A spin coupled to three electrodes with equal chemical potentials: source ($n=1$), drain ($n = 3$), and a gate ($n = 2$), with $V_{k,1;k',3} = V_{k,3;k',1} = V_{k,2;k',2} = V$, else $V_{k,n;k',n'} = 0$, acquires the maximal exponent of 3/4.

[24] T. K. Ng, Phys. Rev. B **54**, 5814 (1996).

[25] O. Hosten *et al.*, Nature **439**, 949 (2006).

[26] I. Bloch, Nature Phys. **1**, 23 (2005).

[27] I. E. Mazets, G. Kurizki, N. Katz, N. Davidson, Phys. Rev. Lett. **94**, 190403 (2005).

[28] G. Hackenbroich, B. Rosenow, H. A. Weidenmuller, Phys. Rev. Lett. **81**, 5896 (1998).